JACS
JOURNAL OF THE AMERICAN CHEMICAL SOCIETY

Communication

pubs.acs.org/JACS

Visible-Light Photoreduction of CO_2 in a Metal–Organic Framework: Boosting Electron–Hole Separation via Electron Trap States

Hai-Qun Xu,[†,‡,#] Jiahua Hu,[†,§,#] Dengke Wang,[∥] Zhaohui Li,[∥] Qun Zhang,[*,†,§] Yi Luo,[†,§] Shu-Hong Yu,[†,‡] and Hai-Long Jiang[*,†,‡]

[†]Hefei National Laboratory for Physical Sciences at the Microscale, [‡]CAS Key Laboratory of Soft Matter Chemistry, Collaborative Innovation Center of Suzhou Nano Science and Technology, Department of Chemistry, and [§]Synergetic Innovation Center of Quantum Information and Quantum Physics, Department of Chemical Physics, Hefei Science Center of CAS, University of Science and Technology of China, Hefei, Anhui 230026, P. R. China

[∥]Research Institute of Photocatalysis, State Key Laboratory of Photocatalysis on Energy and Environment, College of Chemistry, Fuzhou University, Fuzhou 350002, P. R. China

Supporting Information

ABSTRACT: It is highly desirable to convert CO_2 to valuable fuels or chemicals by means of solar energy, which requires CO_2 enrichment around photocatalysts from the atmosphere. Here we demonstrate that a porphyrin-involved metal–organic framework (MOF), PCN-222, can selectively capture and further photoreduce CO_2 with high efficiency under visible-light irradiation. Mechanistic information gleaned from ultrafast transient absorption spectroscopy (combined with time-resolved photoluminescence spectroscopy) has elucidated the relationship between the photocatalytic activity and the electron–hole separation efficiency. The presence of a deep electron trap state in PCN-222 effectively inhibits the detrimental, radiative electron–hole recombination. As a direct result, PCN-222 significantly enhances photocatalytic conversion of CO_2 into formate anion compared to the corresponding porphyrin ligand itself. This work provides important insights into the design of MOF-based materials for CO_2 capture and photoreduction.

Our heavy dependence on fossil fuels for energy results in excessive CO_2 emissions and global warming. Tremendous efforts have been made to address this challenge. Currently, carbon capture and sequestration/separation from post-combustion effluents is an accepted working approach. The captured CO_2 is injected into underground geological formations for permanent sequestration. But catalytic transformation of the captured CO_2 into high-value chemicals and/or fuels would be more desirable than simply storing it as waste. Toward this end, chemical reduction of CO_2 with solar energy is one of the most promising solutions. In the past decades, diverse semiconductors, metal-incorporated zeolites, and metal complexes have been exploited for CO_2 photoreduction,[1] but the molecular systems are mostly limited to expensive noble metal catalysts.[1g] TiO_2-based photocatalysts have been intensively investigated owing to their stability and availability at low cost.[1h,2] Unfortunately, their efficiency for CO_2 photoreduction is not satisfactory, partly because of the weak CO_2 adsorption on the catalyst surface. In addition, most of the reported photocatalysts are active only in the ultraviolet (UV) region. Given that UV light accounts for only ~4% while visible light contributes ~43% of solar energy, it is rather imperative to develop visible-light-responsive photocatalysts.[1f]

To integrate CO_2 capture and its photocatalytic conversion using solar energy, metal–organic frameworks (MOFs),[3] a relatively new class of porous materials, could be a judicious choice. MOFs have been extensively studied over the past two decades and demonstrated to possess promising applications in many fields,[4−6] especially in CO_2 capture,[7] thanks to their high porosity and tunable interaction with CO_2 molecules. In addition, previous studies have revealed that metal clusters in MOFs can behave as inorganic semiconductor quantum entities, and the organic linkers could serve as antenna to activate these metal clusters upon photoexcitation,[8] thus making "MOF-based photocatalysis" possible. Some MOFs have recently been developed for photocatalytic water splitting,[9] but reports on photocatalytic CO_2 reduction using MOFs[10] or MOF-based composites[11] are still very rare. Meanwhile, the catalytic mechanism remains largely unclear. Given the versatile and tailorable characters of MOF structures, the utilization of solar energy by MOFs, especially in the visible region, could be feasible by judiciously selecting metal ions and organic linkers. However, the current modulation of light absorption over MOFs is limited to a narrow range by tethering the ligand with one or two additional amine groups.[10b,c] To efficiently harvest visible light, it is desired to develop MOFs with absorption covering the visible region as widely as possible.

With all these in mind, we have employed a very stable mesoporous zirconium–porphyrin MOF, PCN-222 (also called MOF-545 or MMPF-6), based on tetrakis(4-carboxyphenyl)-porphyrin (H_2TCPP),[12] for effective integration of CO_2 capture and CO_2 reduction under visible-light irradiation in the presence of triethanolamine (TEOA) as a sacrificial agent. The H_2TCPP ligand in PCN-222 behaves as a visible-light-harvesting unit, and the high CO_2 uptake might facilitate the enrichment of CO_2 molecules around the catalytic Zr_6 centers, thereby enhancing the photocatalytic efficiency. Furthermore, interrogations by means of ultrafast spectroscopy (together with time-resolved

Received: April 7, 2015
Published: October 4, 2015

DOI: 10.1021/jacs.5b08773
J. Am. Chem. Soc. 2015, 137, 13440−13443

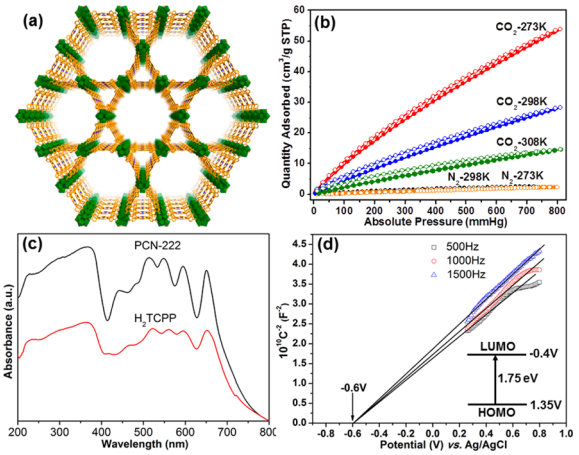

Figure 1. (a) View of the 3D network of PCN-222 featuring large channels running through the *c*-axis. (b) CO_2 and N_2 sorption isotherms of PCN-222 at different temperatures. (c) UV/vis spectra of H_2TCPP and PCN-222. (d) Mott–Schottky plots for PCN-222 in 0.2 M Na_2SO_4 aqueous solution (pH 6.8); inset is the energy diagram of the HOMO and LUMO levels of PCN-222.

photoluminescence (PL) spectroscopy), for the first time on a MOF photocatalyst, have allowed us to unveil the underlying mechanism. We have found that the emergence of a type of deep electron trap state in PCN-222 enables effective suppression of the detrimental electron–hole recombination. Hence, PCN-222 is capable of supplying long-lifetime electrons for the photoreduction of captured CO_2 molecules with much higher activity than that of the H_2TCPP ligand.

Rod-shaped PCN-222, formulated as $Zr_6(\mu_3\text{-}OH)_8(OH)_8(TCPP)_2$, was prepared according to the documented method (Supporting Information (SI), section 2, and Figure S1).[12] PCN-222 exhibits a 3D network based on Zr_6 clusters connected by H_2TCPP ligand and features ultra-large 1D channels of 3.7 nm diameter (Figures 1a and S2). Despite its high N_2 sorption at 77 K and the large BET surface area (~1728 m^2/g, Figure S4), PCN-222 adsorbs little N_2 at 273 or 298 K. In contrast, it shows high CO_2 uptake of 14, 35, and 58 cm^3/g at 308, 298, and 273 K at 1 atm, respectively (Figure 1b). This suggests a sound interaction between the PCN-222 framework and CO_2 molecules. The calculated heat of adsorption for CO_2 is 23.6 kJ/mol, implying that PCN-222 can be readily regenerated with low energy penalty. These features render PCN-222 a suitable material for CO_2 enrichment in a N_2-rich atmosphere.

The UV/vis spectrum of PCN-222, which well inherits the feature of the H_2TCPP ligand, shows a broad, strong absorption in the region of 200–800 nm (Figure 1c). This allows for promoting the electrons of PCN-222 to an excited state upon visible-light irradiation. To elucidate the semiconductor character of PCN-222 and its possibility for subsequent CO_2 photoreduction, Mott–Schottky measurements on PCN-222 were conducted at frequencies of 500, 1000, and 1500 Hz (Figure 1d). The positive slope of the obtained C^{-2} values (vs the applied potentials) is consistent with that of the typical *n*-type semiconductors. The intersection point is independent of the frequency, and the flat band position determined from the intersection is ~ −0.60 V vs Ag/AgCl (i.e., −0.40 V vs NHE). Since it is generally accepted that the bottom of the conduction band (LUMO) in *n*-type semiconductors is approximately equal to the flat-band potential,[13] the LUMO of PCN-222 is estimated to be −0.40 V vs NHE. With the bandgap energy of PCN-222

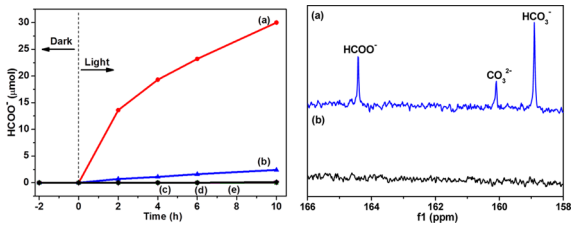

Figure 2. Left: Amount of $HCOO^-$ produced as a function of the time of visible-light irradiation over (a) PCN-222, (b) H_2TCPP, (c) no PCN-222, (d) no TEOA, and (e) no CO_2. The reaction with each photocatalyst (50 mg) in the MeCN/TEOA (10:1 v/v, 60 mL) solution was irradiated using a Xe lamp filtered to produce light in the range of 420–800 nm. Right: ^{13}C NMR spectra for the product obtained from reaction with (a) $^{13}CO_2$ or (b) $^{12}CO_2$.

estimated to be 1.75 eV from the Tauc plot (Figure S5), its valence band (HOMO) is then calculated to be 1.35 V vs NHE (Figure 1d). Given the more negative potential of LUMO in PCN-222 than the reduction potential of CO_2 to formate (−0.28 V vs NHE), it is theoretically feasible for the photocatalytic reduction of CO_2 to generate formate over PCN-222. The Mott–Schottky plot and UV/vis spectrum suggest that the H_2TCPP ligand is able to act as a visible-light-harvesting unit (SI, section 4).

Photocatalytic reduction of CO_2 over PCN-222 was conducted with TEOA in CH_3CN as solvent (due to its good solubility for CO_2 and possible cation-solvating property, beneficial for electron transfer to CO_2[11c,14]) under visible-light irradiation (Figure 2, left). Remarkably, PCN-222 exhibits significant photocatalytic activity for CO_2 reduction. The $HCOO^-$ anion was continuously produced, the amount increasing to 30 μmol in 10 h, much higher than the values observed over UiO-66-NH_2 and MIL-125-NH_2 under similar conditions.[10b,c] No other products can be detected in the gas and liquid phases (Figures S8 and S9), suggesting that the catalyst is highly selective toward the conversion. Examining the stability of PCN-222, recycling experiments demonstrate that no noticeable change in the yield rate of $HCOO^-$ occurs during the three reaction runs (Figure S10). The powder X-ray diffraction profile further manifests that the structure of PCN-222 is retained after reaction (Figure S11). No $HCOO^-$ was detected in the absence of either PCN-222 or TEOA, demonstrating their critical roles in the reaction. Moreover, no $HCOO^-$ was generated when the reaction was carried out in the dark, demonstrating a truly photocatalytic behavior (Figure 2, left). To verify the origin of $HCOO^-$, N_2 instead of CO_2 as a reactant was introduced into the reaction system under otherwise similar conditions. Only a trace amount (0.14 μmol) of $HCOO^-$ was obtained after 10 h. Furthermore, the isotopic $^{13}CO_2$ was employed in the photocatalytic reaction, and the product was identified by ^{13}C NMR spectroscopy to confirm the origin of $HCOO^-$. The ^{13}C NMR spectrum clearly gave a peak at 164.8 ppm, corresponding to $HCOO^-$, when $^{13}CO_2$ was introduced,[10b] while that signal was not detected with $^{12}CO_2$ only (Figure 2, right, and Figures S12 and S13). The results unambiguously demonstrate that the produced $HCOO^-$ anion indeed comes from CO_2. It is safe to conclude that PCN-222 is very active and capable of selectively converting CO_2 to $HCOO^-$ under visible-light irradiation. To unveil the mechanism behind the CO_2 photoreduction over PCN-222, electron spin resonance studies were conducted and revealed that Zr^{III} ions are generated by electron transfer (SI, section 5, and Figure S14). We thus propose that, upon

DOI: 10.1021/jacs.5b08773
J. Am. Chem. Soc. 2015, 137, 13440–13443

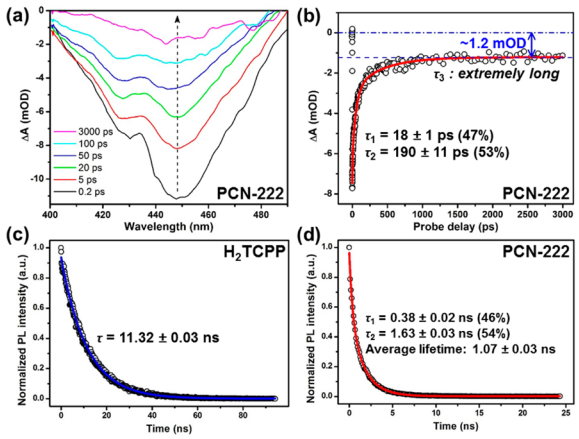

Figure 3. (a) Transient TA spectra of PCN-222 registered at different probe delays (pump at 500 nm). (b) Representative TA kinetics of PCN-222 taken at the probing wavelength of 430 nm. In (a) and (b), the TA signal is given as absorbance change (ΔA) with unit of mOD (OD is optical density). Time-resolved PL kinetics for (c) H_2TCPP and (d) PCN-222, recorded with excitation at 515 nm and emission at 712 nm.

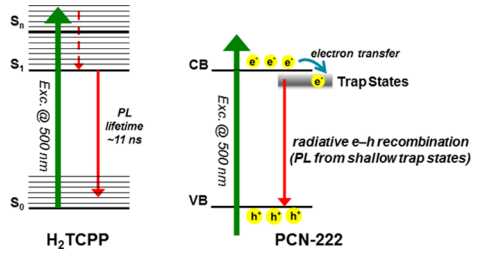

Figure 4. Mechanisms underlying the photoexcited dynamics involved in H_2TCPP (left) and PCN-222 (right). Left: S_0, S_1, and S_n denote the electronic ground state, the first electronically excited state, and a certain high-lying electronically excited state reached by the 500 nm photon, respectively. Right: VB (CB), denoting the valence (conduction) band.

irradiation, the H_2TCPP in PCN-222 behaves as an antenna to absorb visible light to its excited state, which then transfers electrons to the Zr oxo clusters for reduction of CO_2 to $HCOO^-$ in the presence of TEOA as the electron donor (SI, section 5, and Scheme S1).[10b] During this process, TEOA might be oxidized to its aldehyde form (SI, section 6, Scheme S2 and Figure S15).

For comparison, H_2TCPP was also employed as a photocatalyst to reduce CO_2 under similar conditions. Only 2.4 μmol of $HCOO^-$ was produced after 10 h (Figure 2, left, and Table S1), confirming that the photocatalytic activity can be greatly enhanced by assembling the H_2TCPP ligand onto MOFs. Notably, the steady-state PL measurement (Figure S16) indicates that the transformation from H_2TCPP to PCN-222 results in pronounced PL emission quenching, implying greatly suppressed radiative electron−hole recombination in PCN-222 relative to H_2TCPP, in line with the observed higher photocatalytic activity of PCN-222 than H_2TCPP.

To gain a deeper understanding of the efficacy of photoexcited charge separation in PCN-222, we resorted to ultrafast transient absorption (TA) spectroscopy, a robust tool for tracking in real time the charge carrier dynamics in nanosystems.[11b,15] In our TA measurements, a femtosecond visible pump/white-light continuum (WLC) probe scheme was adopted (see SI for details of the pump/probe experiments). The center wavelength of the pump pulses was chosen at 500 nm (i.e., 2.48 eV), which can effectively photoinduce an interband transition in the semiconductor-like PCN-222 system. Figure 3a shows the transient TA spectra recorded at probe delays from 0.2 to 3000 ps, all of which manifest as negative absorbance changes (ΔA) due to ground-state bleaching, noting that the WLC probe (400−490 nm) is blue-shifted relative to the 500 nm pump. As the WLC probe yields essentially the same TA kinetics in this spectral region, we show in Figure 3b a typical spectrum taken at 430 nm. Within the probe-delay limit of our pump/probe spectrometer (~3 ns), the ΔA recovery converges to an asymptote (dashed line in Figure 3b) with a non-zero value of ~ −1.2 mOD. Multiexponential fitting to this asymptotic recovery gives rise to two characteristic time constants, τ_1 = 18 ± 1 ps (47%) and τ_2 = 190 ± 11 ps (53%). Notably, the nearly perfect parallelism between the asymptote and the ΔA = 0 line (dashed-dotted line in Figure 3b) suggests that the eventual recovery to ΔA = 0 (a process that should take place)[15] features an extremely long lifetime (τ_3), probably a few tens to hundreds of nanoseconds or even a microsecond long.

The observed two components in the picosecond domain (τ_1 and τ_2) may reflect the electron dynamics associated with the electron trap states that are energetically located within the bandgap of PCN-222. Considering that the lifetimes of such trap states (characterizing the electron-detrapping rates) are typically in the nanosecond domain,[16] we resorted to time-resolved PL spectroscopy. In Figure 3c,d, we compare the PL kinetics of H_2TCPP and PCN-222 at 712 nm emission (i.e., the maximum for the lower-lying PL band excited at 515 nm; refer to Figure S16). The PL lifetime of H_2TCPP is determined to be 11.32 ± 0.03 ns. Interestingly, similarly to the TA case, two lifetimes with sizable components were also observed for the PL of PCN-222: τ_1 = 0.38 ± 0.02 ns (46%) and τ_2 = 1.63 ± 0.03 ns (54%), or 1.07 ± 0.03 ns on average.

By combining the above TA and PL observations, we illustrate the pertinent mechanisms underlying the photoexcited dynamics involved in the two systems (Figure 4). For the molecular system of H_2TCPP (left panel), the relevant picture is quite straightforward: The 500 nm laser pulse launches an electronic transition from the ground state S_0 to a certain excited state S_n, followed by rapid intramolecular deactivation processes to the lowest-lying excited state S_1, as dictated by Kasha's rule.[17] As a result, PL from S_1 to S_0 with a lifetime of ~11 ns was detected. On the other hand, in the semiconductor-like PCN-222 system (right panel), the existence of two distinct lifetimes for the PL emissions monitored at ~712 nm (i.e., 1.74 eV, slightly below the 1.75 eV bandgap) suggests that the radiative electron−hole recombination could originate from two trap states (acting as PL emission centers)[16] that are located in very close proximity to the conduction band bottom. These two near-band-edge trap states receive and accumulate the photogenerated electrons transferred from the conduction band bottom in a bi-exponential relaxation manner, reflecting their different trap depths. In terms of the bi-exponential component proportions, the two electron-trapping processes (47% for τ_1 and 53% for τ_2) seem to nicely coincide with the PL emissions (46% for τ_1 and 54% for τ_2), providing collateral evidence for the validity of our assignment. As compared to the S_1 state of H_2TCPP, the two trap states of PCN-222 are relatively short-lived (~1 ns on average for PCN-222 vs ~11 ns for H_2TCPP), implying relatively shallow depths. Nevertheless, the eventual recovery (to ΔA = 0) featuring an extremely long lifetime τ_3 most likely correlates to a third trap state having a rather deep depth. The detrapping of electrons from this deep trap state turns out to be so slow that its corresponding radiative electron−hole recombination is dramat-

DOI: 10.1021/jacs.5b08773
J. Am. Chem. Soc. 2015, 137, 13440−13443

ically suppressed, which reasonably explains the absence of the long-lifetime component in the time-resolved PL kinetics (refer to Figure 3d). We thus conclude that, as a direct result of the transformation from H_2TCPP to its MOF architecture (i.e., PCN-222), such a unique, deep trap state emerges and enables effective accumulation of long-lived, photogenerated electrons ready for the photocatalytic reduction of CO_2 molecules captured by PCN-222.

In summary, the photocatalytic reduction of CO_2 under visible-light irradiation has been realized, for the first time, over a photoactive porphyrin-based semiconducting MOF of PCN-222, which exhibits much better activity than the H_2TCPP ligand alone. The high CO_2 uptake capacity in the MOF might allow it to interact better with CO_2 in MeCN, thus benefiting its photocatalytic conversion. Moreover, as demonstrated by ultrafast transient absorption and photoluminescence spectroscopy, the emergence of an extremely long-lived electron trap state in PCN-222 substantially suppresses the detrimental electron−hole recombination, thereby boosting the efficiency of the CO_2 photoreduction. The current study highlights the great potential and advantages in the assembly of a photoactive molecular system, such as porphyrin, into MOFs for CO_2 photoreduction. This work not only provides a deeper understanding of the electron-transfer mechanism involved in MOFs but also should stimulate further studies toward developing more efficient visible-light-responsive MOFs for CO_2 capture and photoreduction utilizing solar energy.

■ ASSOCIATED CONTENT

Supporting Information

The Supporting Information is available free of charge on the ACS Publications website at DOI: 10.1021/jacs.5b08773.

Experimental details and characterization data (PDF)

■ AUTHOR INFORMATION

Corresponding Authors

*jianglab@ustc.edu.cn

*qunzh@ustc.edu.cn

Author Contributions

#H.-Q.X. and J.H. contributed equally to this work.

Notes

The authors declare no competing financial interest.

■ ACKNOWLEDGMENTS

We are grateful to the reviewers for their insightful comments and valuable suggestions, and Prof. Z. Wang at Troy Univ. for helpful discussions. This work was supported by the 973 program (2014CB931803, 2010CB923300, 2014CB239303), the NSFC (21371162, 21521001, 21173205, 91127042, 21273035), the CAS (XDB01020000), the Recruitment Program of Global Youth Experts, and the Fundamental Research Funds for the Central Universities (WK2060190026, WK2340000063).

■ REFERENCES

(1) (a) Inoue, T.; Fujishima, A.; Konishi, S.; Honda, K. *Nature* **1979**, *277*, 637. (b) Matsuoka, M.; Anpo, M. *J. Photochem. Photobiol., C* **2003**, *3*, 225. (c) Indrakanti, V. P.; Kubicki, J. D.; Schobert, H. H. *Energy Environ. Sci.* **2009**, *2*, 745. (d) Liu, Q.; Zhou, Y.; Kou, J.; Chen, X.; Tian, Z.; Gao, J.; Yan, S.; Zou, Z. *J. Am. Chem. Soc.* **2010**, *132*, 14385. (e) Iizuka, K.; Wato, T.; Miseki, Y.; Saito, K.; Kudo, A. *J. Am. Chem. Soc.* **2011**, *133*, 20863. (f) Tong, H.; Ouyang, S. X.; Bi, Y. P.; Umezawa, N.; Oshikiri, M.; Ye, J. H. *Adv. Mater.* **2012**, *24*, 229. (g) Sato, S.; Morikawa, T.; Kajino, T.; Ishitani, O. *Angew. Chem., Int. Ed.* **2013**, *52*, 988. (h) Habisreutinger, S. N.; Schmidt-Mende, L.; Stolarczyk, J. K. *Angew. Chem., Int. Ed.* **2013**, *52*, 7372.

(2) Dhakshinamoorthy, A.; Navalon, S.; Corma, A.; Garcia, H. *Energy Environ. Sci.* **2012**, *5*, 9217.

(3) (a) Long, J. R.; Yaghi, O. M. *Chem. Soc. Rev.* **2009**, *38*, 1213. (b) Zhou, H.-C.; Long, J. R.; Yaghi, O. M. *Chem. Rev.* **2012**, *112*, 673. (c) Furukawa, H.; Cordova, K. E.; O'Keeffe, M.; Yaghi, O. M. *Science* **2013**, *341*, 974. (d) Zhou, H.-C.; Kitagawa, S. *Chem. Soc. Rev.* **2014**, *43*, 5415.

(4) (a) Suh, M. P.; Park, H. J.; Prasad, T. K.; Lim, D.-W. *Chem. Rev.* **2012**, *112*, 782. (b) He, Y.; Zhou, W.; Qian, G.; Chen, B. *Chem. Soc. Rev.* **2014**, *43*, 5657. (c) Van de Voorde, B.; Bueken, B.; Denayer, J.; De Vos, D. *Chem. Soc. Rev.* **2014**, *43*, 5766.

(5) (a) Lee, J.; Farha, O. K.; Roberts, J.; Scheidt, K. A.; Nguyen, S. T.; Hupp, J. T. *Chem. Soc. Rev.* **2009**, *38*, 1450. (b) Farrusseng, D.; Aguado, S.; Pinel, C. *Angew. Chem., Int. Ed.* **2009**, *48*, 7502. (c) Jiang, H.-L.; Xu, Q. *Chem. Commun.* **2011**, *47*, 3351. (d) Gascon, J.; Corma, A.; Kapteijn, F.; Llabrés i Xamena, F. X. *ACS Catal.* **2014**, *4*, 361. (e) Zhang, T.; Lin, W. *Chem. Soc. Rev.* **2014**, *43*, 5982.

(6) (a) Horike, S.; Shimomura, S.; Kitagawa, S. *Nat. Chem.* **2009**, *1*, 695. (b) Lin, R.-B.; Li, F.; Liu, S.-Y.; Qi, X.-L.; Zhang, J.-P.; Chen, X.-M. *Angew. Chem., Int. Ed.* **2013**, *52*, 13429.

(7) Sumida, K.; Rogow, D. L.; Mason, J. A.; McDonald, T. M.; Bloch, E. D.; Herm, Z. R.; Bae, T.-H.; Long, J. R. *Chem. Rev.* **2012**, *112*, 724.

(8) (a) Alvaro, M.; Carbonell, E.; Ferrer, B.; Llabrés i Xamena, F. X.; Garcia, H. *Chem. - Eur. J.* **2007**, *13*, 5106. (b) Tachikawa, T.; Choi, J. R.; Fujitsuka, M.; Majima, T. *J. Phys. Chem. C* **2008**, *112*, 14090.

(9) (a) Kataoka, Y.; Sato, K.; Miyazaki, Y.; Masuda, K.; Tanaka, H.; Naito, S.; Mori, W. *Energy Environ. Sci.* **2009**, *2*, 397. (b) Silva, C. G.; Luz, I.; Llabrés i Xamena, F. X.; Corma, A.; García, H. *Chem. - Eur. J.* **2010**, *16*, 11133. (c) Fateeva, A.; Chater, P. A.; Ireland, C. P.; Tahir, A. A.; Khimyak, Y. Z.; Wiper, P. V.; Darwent, J. R.; Rosseinsky, M. J. *Angew. Chem., Int. Ed.* **2012**, *51*, 7440. (d) Wang, C.; deKrafft, K. E.; Lin, W. *J. Am. Chem. Soc.* **2012**, *134*, 7211. (e) Pullen, S.; Fei, H.; Orthaber, A.; Cohen, S. M.; Ott, S. *J. Am. Chem. Soc.* **2013**, *135*, 16997. (f) Zhou, T.; Du, Y.; Borgna, A.; Hong, J.; Wang, Y.; Han, J.; Zhang, W.; Xu, R. *Energy Environ. Sci.* **2013**, *6*, 3229. (g) Sasan, K.; Lin, Q.; Mao, C.; Feng, P. *Chem. Commun.* **2014**, *50*, 10390. (h) Saha, S.; Das, G.; Thote, J.; Banerjee, R. *J. Am. Chem. Soc.* **2014**, *136*, 14845.

(10) (a) Wang, C.; Xie, Z.; deKrafft, K. E.; Lin, W. *J. Am. Chem. Soc.* **2011**, *133*, 13445. (b) Fu, Y.; Sun, D.; Chen, Y.; Huang, R.; Ding, Z.; Fu, X.; Li, Z. *Angew. Chem., Int. Ed.* **2012**, *51*, 3364. (c) Sun, D.; Fu, Y.; Liu, W.; Ye, L.; Wang, D.; Yang, L.; Fu, X.; Li, Z. *Chem. - Eur. J.* **2013**, *19*, 14279. (d) Li, L.; Zhang, S.; Xu, L.; Wang, J.; Shi, L.-X.; Chen, Z.-N.; Hong, M.; Luo, J. *Chem. Sci.* **2014**, *5*, 3808. (e) Lee, Y.; Kim, S.; Kang, J. K.; Cohen, S. M. *Chem. Commun.* **2015**, *51*, 5735.

(11) (a) Liu, Q.; Low, Z.-X.; Li, L.; Razmjou, A.; Wang, K.; Yao, J.; Wang, H. *J. Mater. Chem. A* **2013**, *1*, 11563. (b) Li, R.; Hu, J.; Deng, M.; Wang, H.; Wang, X.; Hu, Y.; Jiang, H.-L.; Jiang, J.; Zhang, Q.; Xie, Y.; Xiong, Y. *Adv. Mater.* **2014**, *26*, 4783. (c) Wang, S.; Yao, W.; Lin, J.; Ding, Z.; Wang, X. *Angew. Chem., Int. Ed.* **2014**, *53*, 1034.

(12) (a) Feng, D.; Gu, Z.-Y.; Li, J.-R.; Jiang, H.-L.; Wei, Z.; Zhou, H.-C. *Angew. Chem., Int. Ed.* **2012**, *51*, 10307. (b) Morris, W.; Volosskiy, B.; Demir, S.; Gándara, F.; McGrier, P. L.; Furukawa, H.; Cascio, D.; Stoddart, J. F.; Yaghi, O. M. *Inorg. Chem.* **2012**, *51*, 6443. (c) Chen, Y.; Hoang, T.; Ma, S. *Inorg. Chem.* **2012**, *51*, 12600.

(13) (a) Zhang, Z.; Long, J.; Yang, L.; Chen, W.; Dai, W.; Fu, X.; Wang, X. *Chem. Sci.* **2011**, *2*, 1826. (b) Maeda, K.; Sekizawa, K.; Ishitani, O. *Chem. Commun.* **2013**, *49*, 10127.

(14) Matsuoka, S.; Kohzuki, T.; Pac, C.; Ishida, A.; Takamuku, S.; Kusaba, M.; Nakashima, N.; Yanagida, S. *J. Phys. Chem.* **1992**, *96*, 4437.

(15) (a) Hannaford, P. *Femtosecond Laser Spectroscopy*; Springer: New York, 2005. (b) Wu, K.; Zhu, H.; Liu, Z.; Rodríguez-Córdoba, W.; Lian, T. *J. Am. Chem. Soc.* **2012**, *134*, 10337. (c) Zhang, Q.; Zheng, H.; Geng, Z.; Jiang, S.; Ge, J.; Fan, K.; Duan, S.; Chen, Y.; Wang, X.; Luo, Y. *J. Am. Chem. Soc.* **2013**, *135*, 12468.

(16) Wheeler, D. A.; Zhang, J. Z. *Adv. Mater.* **2013**, *25*, 2878.

(17) Kasha, M. *Discuss. Faraday Soc.* **1950**, *9*, 14.

DOI: 10.1021/jacs.5b08773
J. Am. Chem. Soc. 2015, 137, 13440−13443